

**Mapping the ultrafast dynamics of adenine onto its nucleotide and
oligonucleotides by time-resolved photoelectron imaging**

Adam S. Chatterley,^{1,2} Christopher W. West,¹ Gareth M. Roberts,² Vasilios G. Stavros,² and Jan R.

R. Verlet^{1}*

¹Department of Chemistry, University of Durham, Durham DH1 3LE, UK

²Department of Chemistry, University of Warwick, Coventry CV4 7AL, UK

**Correspondence: j.r.r.verlet@durham.ac.uk*

Abstract

The intrinsic photo-physics of nucleobases and nucleotides following UV absorption presents a key reductionist step towards understanding the complex photo-damage mechanisms occurring in DNA. Adenine in particular has been the focus of intense investigation, where there has been a long-standing uncertainty about the mechanism and how the dynamics of adenine correlate to those of its more biologically relevant nucleotide and oligonucleotides in aqueous solution. Here we report on time-resolved photoelectron imaging of the deprotonated 3'-deoxy-adenosine-5'-monophosphate nucleotide and the adenosine di- and tri-nucleotides. Through a comparison of gas and solution phase experiments and available theoretical studies, we show that the dynamics of the base are insensitive to the surrounding environment and that the decay of the adenine base within a nucleotide probably involves internal conversion from the initially populated $^1\pi\pi^*$ states. This is in agreement with some recent theoretical studies. The relaxation dynamics of the adenosine oligonucleotides are very similar to those of the nucleobase, in contrast to the aqueous oligonucleotides, where a fraction of the ensemble forms long-lived excimer states that are delocalised over two bases.

The absorption of ultraviolet (UV) radiation by DNA can lead to biological damage including strand breaks and mutations that can ultimately lead to photolesions, transcription errors and cancer.¹ Despite the efficient UV absorption, mediated by the optically bright $^1\pi\pi^*$ states localised on the four DNA nucleobases, the photodamage quantum yield in DNA is low (<1%).^{2,3} This photostability is governed by the non-radiative decay mechanisms that enable the nucleobases to assimilate and dispose of the potentially harmful electronic energy in a non-destructive fashion. Gaining a molecular level understanding of these processes has been a long-standing goal, not only because of its role in radiation damage of DNA, but also to assess why nature has evolved using such a select number of molecular building blocks to define the genetic code.⁴

Much of the experimental effort has been devoted to the fate of adenine (Ade) following excitation to its $^1\pi\pi^*$ states. Gas-phase spectroscopy⁵⁻¹¹ synergised with theoretical calculations¹²⁻¹⁷ in particular has provided deep insight. However, there remains disagreement about the basic radiationless decay mechanism and, in particular, how the dynamics of Ade relate to those of its more biologically relevant nucleotide and oligonucleotides in aqueous solution. Although ultrafast spectroscopy on aqueous phase nucleotides probes the more relevant environments, such experiments generally come at the cost of the detail that can be attained through the gas-phase. In order to bridge the gap between the isolated Ade base and solvated nucleotides, we have performed experiments on the isolated nucleotide. Specifically, we use electrospray ionisation (ESI) to generate deprotonated 3'-deoxy-adenosine-5'-monophosphate (dAMP⁻, Fig. 1a) and employ time-resolved photoelectron imaging as a means of probing the dynamics of the *neutral* Ade nucleobase in this environment. Our result enables a comparison between previous studies carried out in the gas and in solution phases as well as with the extensive theoretical studies. This body of data allows the influence of the environment on the excited state dynamics to be probed and provides insights into the most likely decay mechanism.

A key result is that the dynamics of Ade appear to correlate closely to those of its nucleotide, regardless of whether it is solvated or not. This is in agreement with some theoretical

predictions and suggestions that the excited state dynamics proceed primarily on a single excited state.^{14,18-20} But how do the base dynamics extend to larger oligomeric systems? In aqueous solution, new mechanisms become accessible, which occur alongside apparently monomeric dynamics.^{2,3} Although these competing processes have attracted much recent attention, their dynamics can obscure those due to single bases in the nucleotide, which is at the heart of understanding how the base dynamics evolve with size and remains one of the most important photoprotection mechanisms in DNA.²¹ In order to explore this evolution we have also extended our studies to isolated adenosine di- and tri-nucleotides.

Experiments were conducted using our femtosecond anion photoelectron imaging spectrometer, which has been described in detail previously,²²⁻²⁴ and combines ESI with velocity-map imaging.²⁵ dAMP⁻ anions were produced by ESI at -2.5 kV from a ~1 mM solution of dAMP sodium salt (98% Sigma-Aldrich) in methanol, and oligonucleotide anions were produced by ESI from a ~0.5 mM solution of the oligonucleotide (desalted, Sigma-Aldrich) in methanol. The anions were transferred into vacuum, accumulated in a ring-electrode ion trap, and packets ejected at 50 Hz repetition rate into a collinear time-of-flight mass-spectrometer. The mass-selected ion packet was intersected in the centre of a velocity-map imaging setup by femtosecond pump and probe laser pulses. Detached photoelectrons were directed onto a position sensitive detector and photoelectron images typically collected for 5×10^4 laser shots per pump-probe delay. For each delay, a photoelectron image acquired for an equal number of laser shots without ions was subtracted, to remove background photoelectron noise induced by the 266 nm light. Raw images were deconvoluted using the polar onion-peeling algorithm.²⁶ The energy resolution is $\Delta eKE/eKE \sim 5\%$ and spectra have been calibrated to the well-known spectrum of iodide.

Femtosecond laser pulses were derived from a commercial Ti:Sapphire oscillator and amplifier laser, centred at 1.55 eV (800 nm). The 4.66 eV (266 nm) pump pulses were generated using two type I beta-barium borate (BBO) crystals, firstly to produce 3.10 eV (400 nm) light using second harmonic generation, followed by sum frequency generation to mix the 3.10 eV photons

with the 1.55 eV fundamental. The 3.10 eV (400 nm) probe pulses were generated using a further type I BBO crystal. Probe pulses were delayed with respect to the pump using a motorised optical delay line. Pump and probe beams were combined collinearly using a dichroic mirror and loosely focused into the interaction region with a curved mirror. The intensity of both beams was below 10^{11} W cm⁻². The cross-correlation of the pump and probe pulses was approximately 120 fs, providing a temporal resolution of ~60 fs.

To support our measurements, density functional theory (DFT) and time-dependent DFT (TD-DFT) calculations on both nucleotide anions and nucleobases (as well as Ade-9Me) were performed using the PBE0 functional²⁷ in the Gaussian09 computational suite.²⁸ The functional has been selected for its balanced and robust description of both valence and Rydberg excited states in TD-DFT calculations.²⁹ All vertical excitation energies were calculated at the PBE0/aug-cc-pVDZ//TD-PBE0/aug-cc-pVTZ level of theory. Optimised ground state geometries were confirmed to be (local) minima, as verified through further harmonic frequency calculations (no imaginary frequencies). The effects of a water solvent were simulated using a polarisable continuum model (PCM).

Time-resolved photoelectron spectra for dAMP⁻ are shown as a false colour plot in Fig. 1b. In this, the two-photon contribution from the pump only has been subtracted, which recovers the pump-probe excited state signal because the probe is not resonant with any initial transition. An increase in photoelectron yield at $t = 0$ is observed as population is transferred to the ¹ $\pi\pi^*$ states by the pump. Inspection of the spectra shows two dominant features: at electron kinetic energies, $eKE < 0.7$ eV, there is a component which decays over the course of hundreds of femtoseconds, while between $1 < eKE < 2$ eV, a feature decays within the instrument response.

Quantitative insight can be gained by employing a global fitting procedure,³⁰ whereby the time-resolved photoelectron spectra, $S(eKE, t)$, are fit simultaneously in energy and time by the following equation:

$$S(eKE, t) = \sum_i k_i(eKE) [\exp(-t / \tau_i) * g(t)]$$

where $k_i(eKE)$ is the decay-associated spectrum which is the i^{th} spectral feature that is decaying exponentially with a lifetime, τ_i . The instrument response function was represented by a Gaussian, $g(t)$. Support plane analysis was used to estimate confidence intervals at the 95% level, and the greater of the upper and lower bounds has been reported as the error.

The results of the global fit are shown in Fig. 1c. Only two exponential functions with lifetimes $\tau_1 < 60$ fs and $\tau_2 = 290 \pm 50$ fs are required to fully recover the data (residuals are shown in Fig. S1); the corresponding decay-associated spectra are shown in Fig. 1d. Actual τ_1 lifetimes obtained from the fit are shown Fig. 1, but are limited by our time-resolution of ~ 60 fs. The spectrum of the fast decay, $k_1(eKE)$, shows a peak between $0.7 < eKE < 2$ eV, but is negative for $eKE < 0.5$ eV. Negative signals point to a concomitant exponential rise with a time-constant of τ_1 ; thus, signal that was initially contributing to the $0.7 < eKE < 2$ eV feature is decaying *into* a feature at $eKE < 0.5$ eV. The dynamics are sequential and the initial spectral peak around $0.7 < eKE < 2$ eV decays to form the decay-associated spectrum $k_2(eKE)$, which subsequently decays in a timescale of $\tau_2 = 290$ fs.

The time-resolved photoelectron spectroscopy following excitation at 4.66 eV of Ade and a derivative, Ade-9Me (in which the H atom at the N9 position has been methylated, see Fig. 2), has been performed by Stolow and co-workers and the analysis used was as done here.^{5,7,8} Their study had shown that the dissociative $^1\pi\sigma^*$ state, which is localised on the N9–H bond, may be involved in the decay dynamics of Ade but not Ade-9Me. This was discerned from the shape of the decay-associated spectra which showed additional features due to the $^1\pi\sigma^*$ state. Comparison of the decay-associated spectra for dAMP⁻ (Fig. 1d) with those of Ade-9Me (see Fig. S3) shows striking similarities suggesting that: (i) the $^1\pi\sigma^*$ state is not involved in the decay of dAMP⁻ following excitation at 4.66 eV; and (ii) the dynamics of dAMP⁻ are similar to those in Ade-9Me. The measured $\tau_2 = 1.1$ ps for Ade-9Me is, however, considerably longer than that observed here. This

could be accounted for by the fact that those experiments were performed in a cold molecular beam as opposed to our ions, which are at room temperature or slightly higher. Under our conditions, the internal energy available in the ground state amounts to > 0.46 eV. Hence, several low-frequency modes will be excited and these can greatly accelerate excited state dynamics. We note that Ade-9Me in aqueous solution has a τ_2 lifetime of 220 fs at 263 nm.³ It is of considerable interest to explore the effect of temperature on the excited state dynamics in dAMP⁻ and such experiments are currently being setup in our labs.

The sequential dynamics of Ade-9Me had been interpreted to proceed via a two-step model in which $i = 1$ and $i = 2$, were assigned to the $^1\pi\pi^* \rightarrow ^1n\pi^*$ and $^1n\pi^* \rightarrow S_0$ internal conversion processes, respectively.⁸ Several *ab initio* calculations have also been performed (see ref. 12 and references therein). Although results depend critically on the level of theory, most recent studies indicate that the $^1n\pi^*$ state is not directly involved, contradicting the experimental interpretation.^{14,20} However, the situation is complicated by the prediction that the $^1n\pi^*$ and the $^1\pi\pi^*$ states become strongly mixed along the coordinates leading to two conical intersections.³¹ These involve puckering of the ring at either the C2 or C6 position, as labelled in Fig. 2. A similar mechanism has been proposed for aqueous dAMP⁻, for which there seems to be a general consensus.^{2,3,32} For aqueous Ade, theoretical studies suggests a slightly different mechanism because the strong vibronic coupling in the Franck-Condon regime leads to excitation of both $^1\pi\pi^*$ states and the low-lying $^1n\pi^*$ state.^{33,34} The first lifetime has been associated with decay from S_n to S_1 and the second with decay from the S_1 state. The geometry of the conical intersections were found to be similar between solution and gas-phase.³³

The dynamics of dAMP⁻ have been measured by transient absorption and fluorescence up-conversion in aqueous solution by a number of groups,^{2,3,32} and recently time-resolved photoelectron spectroscopy of solvated adenosine has been reported.³⁵ The most recent solution-phase measurements reported a biexponential decay with lifetimes of the slower ($i = 2$) component as $\tau_2 = 340$ fs for dAMP⁻ (following excitation at 260 nm).³² Given the differences in environments

and experimental techniques, the agreement of this timescale with our results is remarkable. It suggests that the charge localised on the phosphate – which is completely screened in solution^{36,37} – has little or no effect on the dynamics of the base in the gas-phase. This is an important observation as it essentially allows us to view the charged phosphate as a spectator. It also suggests that the hydration of the nucleobase appears to have a small impact on the relaxation dynamics observed experimentally.

The above arguments lead us to conclude that the dynamics of the nucleobase appear to be relatively insensitive to the environment. However, what is the impact of the environment on the excited states, and can this provide any insight into the deactivation mechanism? To gain some insight into this question, we have performed TD-DFT calculations. Our choice of methodology is not to provide quantitative agreement with experiment as there are much higher level calculations in the literature, but rather to gain insight into the *relative* changes between Ade in the differing environments. In Fig. 2 (Table S1), the energies of the relevant excited states are shown for Ade in: isolation, water, nucleotide, and aqueous nucleotide. These trends are in agreement with high-level *ab initio* calculations.^{18,19,31,33}

Our calculations together with the available literature show that the energy of the $^1\pi\sigma^*$ state associated with the N9 position increases in energy in dAMP^- relative to Ade and Ade-9Me, suggesting that this state is not involved in the decay of dAMP^- . However, it is the relative ordering between the $^1\pi\pi^*$ to $^1n\pi^*$ states that is most revealing about the probable decay mechanism. With reference to Fig. 2, in Ade, the $^1n\pi^*$ state lies below the $^1\pi\pi^*$ state, whereas in dAMP^- this ordering is reversed. The effect of solvation is to increase the energy gap between the $^1\pi\pi^*$ and $^1n\pi^*$ states in dAMP^- . One would anticipate that, if the $^1n\pi^*$ state was an intermediate in the decay pathway, the presence of the sugar and phosphate and the effect of solvation on the dynamics would be marked. But this is not the case. Hence, the dynamics in dAMP^- appear not to involve the $^1n\pi^*$ state and are instead dominated by a $^1\pi\pi^* \rightarrow S_0$ internal conversion mechanism. This conclusion is in agreement with some theoretical studies that have stressed a similar independence on environment and a

pathway dominated by the $^1\pi\pi^* \rightarrow S_0$ internal conversion mechanism.^{18,31} On the other hand, in solution, strong mixing of state character often prevents a strict diabatic label from being applied.³³ This makes definitive assignment of mechanism difficult.

In our experiments on $dAMP^-$, we cannot determine the amount of mixing of the $^1n\pi^*$ state along the decay pathway, although it is worth noting that we observe no changes in the photoelectron anisotropy during the decay, which is consistent with dynamics occurring on a single excited state.²³ Our tentative conclusion that the dynamics do not directly involve the $^1n\pi^*$ state is consistent with those reached for solvated deoxyadenosine,³¹ and with certain high-level calculations on solvated Ade:^{18,19} the biexponential dynamics observed are a consequence of motion away from the Franck-Condon region towards conical intersections followed by internal conversion. We note that such biexponential decay has been observed in time-resolved photoelectron spectroscopy for dynamics that are occurring strictly on a single surface,³⁰ indicating that such data are not a prerequisite for the decay through multiple excited states. Finally, in our discussion above and in Fig. 2, we have focussed on the bright $^1\pi\pi^*$ state. There are in fact two close-lying $^1\pi\pi^*$ states in the relevant energy window (see supporting information). However, when considering the other $^1\pi\pi^*$ state, the conclusion about the inactivity of the $^1n\pi^*$ state in the relaxation mechanism is not altered. Nevertheless, we note that in principle both $^1\pi\pi^*$ states can participate, especially in $dAMP^-$, where we have calculated the ordering between the two $^1\pi\pi^*$ states to change.

Above, we have shown the progression of the dynamics in going from isolated Ade through to $dAMP^-$ in aqueous solution. But how do these dynamics evolve in oligonucleotides? ESI provides a straightforward route to the generation of larger complexes in the gas-phase and we present studies on the dynamics of $d(A)_2^-$ and $d(A)_3^-$. Their chemical structures are shown in Fig. 1e and i, together with their time-resolved photoelectron spectra, Fig. 1f and j, respectively. A similar analysis of the time-resolved spectra yielded lifetimes of $\tau_1 < 60$ fs and $\tau_2 = 340 \pm 90$ fs for $d(A)_2^-$

and $\tau_1 < 60$ fs and $\tau_2 = 380 \pm 120$ fs for $d(A)_3^-$. The decay associated spectra are shown in Fig. 1h and l for $d(A)_2^-$ and $d(A)_3^-$, respectively.

Our results show that the ultrafast dynamics of the di- and tri-nucleotide are very similar to that of the mononucleotide (Fig. 1a-d). Indeed, in aqueous solution, “monomer-like” dynamics have also been reported for $d(A)_n^-$ ($n \geq 2$). However, these were convoluted with the dynamics of much longer-lived excited states.^{38,39} Because of this, it has been difficult to exclusively identify the precise nature of these monomer-like dynamics in solution. It has been suggested that differences in the relaxation of a single Ade nucleobase in $d(A)_n^-$ relative to $dAMP^-$ may be caused by sterically hindered conformations or to adjacent bases evolving into the long-lived states.^{2,3,32} From our results on isolated oligonucleotides, the localised dynamics on the Ade base are only mildly influenced by the environment. There is a small increase in lifetime of 40 – 50 fs upon sequential addition of bases in the oligonucleotides. The spectral broadening observed between $d(A)_2^-$ and $d(A)_3^-$ can be correlated with the fact that the charged phosphate is on average further away from one of the nucleobases (see Fig. 1i), which will raise the vertical detachment energy and thus cause a red-shift in the eKE . The maximum eKE remains the same because the other two bases are approximately at the same distance from the charge as in $d(A)_2^-$. The observed decrease in the maximum eKE by ~ 0.2 eV for the oligonucleotides relative to $dAMP^-$ is likely a result of a more effective screening of the charge in the larger systems or may reflect interactions between the nucleobases.³⁶

In solution, additional long-lived dynamics (10s - 100s ps) observed in transient absorption spectra of $d(A)_n^-$ ($n \geq 2$) have been assigned to the formation of excimer states that are delocalised over two (or more) adjacent π -stacked bases.^{2,3,38-40} In our data, no evidence for the formation of long-lived states, excimer or otherwise has been observed. There may be several reasons for the lack of excimer dynamics observed. (i) The fraction of $d(A)_2^-$ or $d(A)_3^-$ that are in a stacked configuration is too low. Our experiments are performed with an internal energy of ~ 300 K and the entropic cost for stacking is likely to be too high compared to the energy gain from π -stacking. In

solution, stacking is favoured because of the unfavourable interaction of the nucleobase with water. The Bowers group have shown that only 65 % of $d(A)_2^-$ were stacked at 80 K using ion mobility.⁴¹

(ii) It is also possible that excimer states are formed but these cannot be observed due to our limited detachment window with the 3.1 eV probe pulses. However, time-resolved photoelectron spectroscopy on $(Ade)_2(H_2O)_3$ clusters would suggest that this is not a problem.⁴² Moreover, our data show a weak but discernible 2-photon ionisation peak, which has a combined probe energy exceeding the ionisation energy of the base (see Fig. S2 in Supplementary Materials). (iii) Finally, it is plausible that a sub-population of the ensemble is stacked but that the excimer states simply cannot form in the gas-phase because of the nearby charge on the phosphate. Recent experiments on a dinucleotide containing Ade and thymine showed a clear signature of charge-transfer character of the long-lived state,⁴³ and this may be destabilised by the Coulomb interaction with an unscreened negative charge. For sufficiently large oligonucleotides or for water-clustered oligonucleotides, this possible destabilisation would diminish.

Supporting Information

Analysis and residuals of global fitting. Comparison of Ade and dAMP⁻ spectra. Theoretical details and results. This material is available free of charge via the internet at <http://pubs.acs.org>

Acknowledgements

We are grateful to Prof. Martin Paterson (Heriot-Watt) for the use of his computing facilities. The project was funded by the Leverhulme Trust (F/00215/BH) and the EPSRC (EP/D073472/1). VGS thanks the Royal Society for a University Research Fellowship. JRRV is grateful to the European Research Council for a Starting Grant (306536).

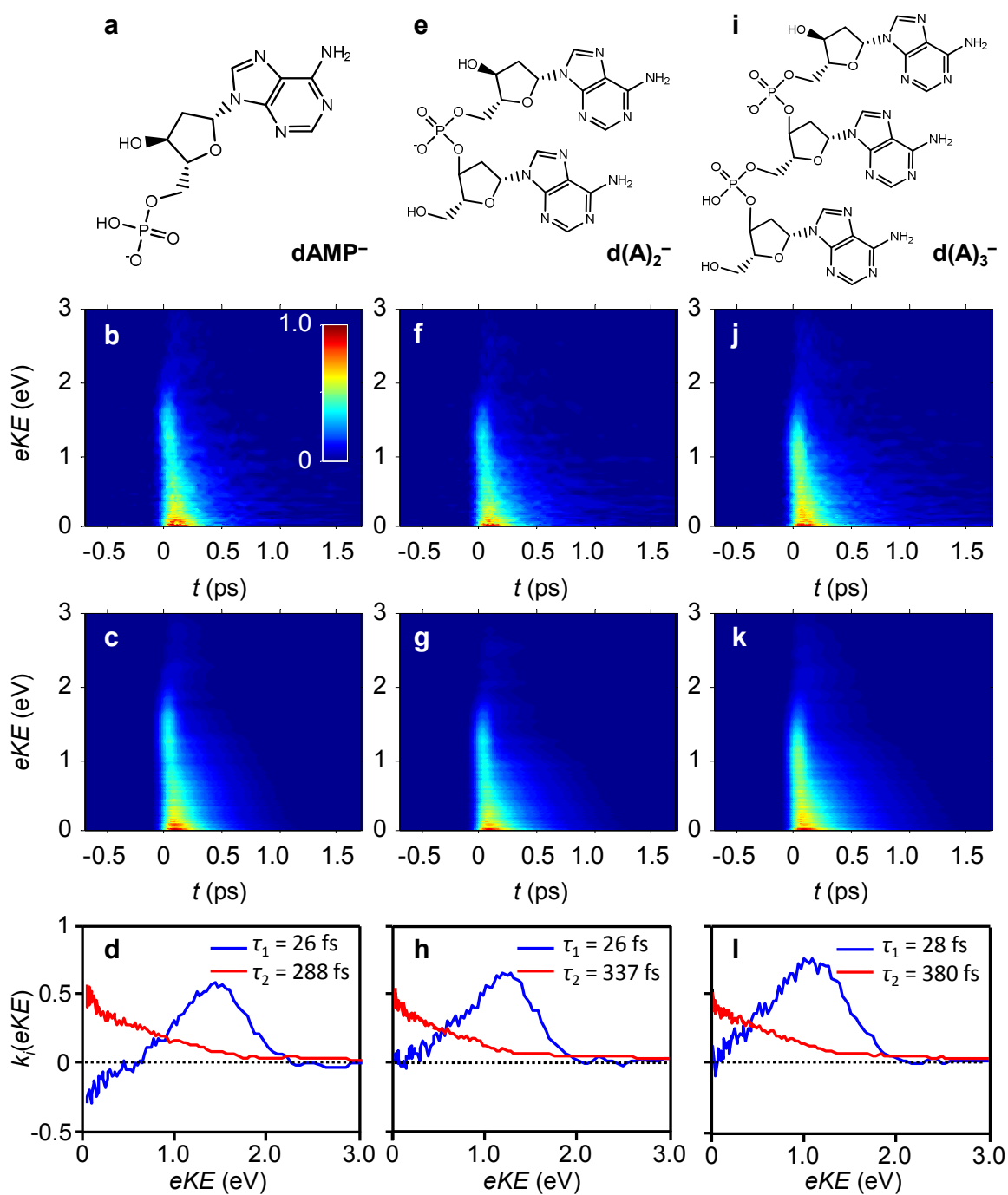


Figure 1 Time-resolved photoelectron spectra of dAMP⁻, d(A)₂⁻ and d(A)₃⁻. a, Chemical structure of dAMP⁻; b, False-colour representation of the time-resolved photoelectron spectra of dAMP⁻ excited at 4.66 eV and probed at 3.10 eV; c, Global fit to the experimental data in b, modelled with two exponential decay functions (see text); d, Decay associated spectra from the global fit in c, showing the spectra of the two decay processes with associated lifetimes indicated. e – h and i – l shows the same as a – d but for d(A)₂⁻ and d(A)₃⁻, respectively.

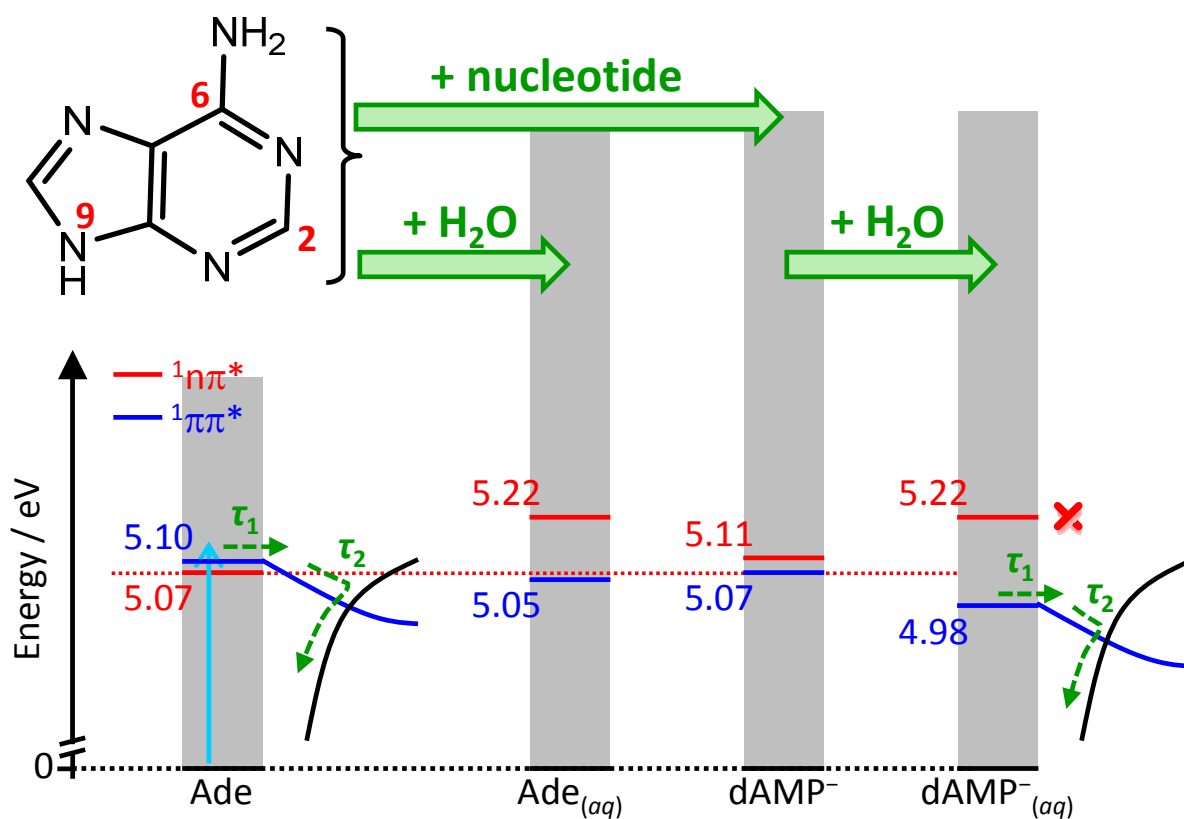


Figure 2 Variations in the calculated vertical excitation energies of Ade in various environments. The relative energies of the $^1n\pi^*$ and $^1\pi\pi^*$ states are indicated. The Franck-Condon region is shown as a grey shaded area. In differing environments, these change substantially although the observed dynamics do not, which suggests that all dynamics are occurring along a single excited state and τ_1 is associated with motion away from the Franck-Condon region, while τ_2 is associated with internal conversion to the ground state (black). Key atoms are labelled for Ade.

References

- (1) Schreier, W. J.; Schrader, T. E.; Koller, F. O.; Gilch, P.; Crespo-Hernández, C. E.; Swaminathan, V. N.; Carell, T.; Zinth, W.; Kohler, B. *Science* **2007**, *315*, 625-629.
- (2) Middleton, C. T.; de La Harpe, K.; Su, C.; Law, Y. K.; Crespo-Hernández, C. E.; Kohler, B. *Annu. Rev. Phys. Chem.* **2009**, *60*, 217-239.
- (3) Crespo-Hernández, C. E.; Cohen, B.; Hare, P. M.; Kohler, B. *Chem. Rev.* **2004**, *104*, 1977-2020.
- (4) Sagan, C. *J. Theor. Biol.* **1973**, *39*, 195-200.
- (5) Ullrich, S.; Schultz, T.; Zgierski, M. Z.; Stolow, A. *J. Am. Chem. Soc.* **2004**, *126*, 2262-2263.
- (6) Canuel, C.; Mons, M.; Piuizzi, F.; Tardivel, B.; Dimicoli, I.; Elhanine, M. *J. Chem. Phys.* **2005**, *122*, 074316-074316.
- (7) Satzger, H.; Townsend, D.; Zgierski, M. Z.; Patchkovskii, S.; Ullrich, S.; Stolow, A. *Proc. Natl. Acad. Sci. USA* **2006**, *103*, 10196-10201.
- (8) Bisgaard, C. Z.; Satzger, H.; Ullrich, S.; Stolow, A. *ChemPhysChem* **2009**, *10*, 101-110.
- (9) Wells, K. L.; Hadden, D. J.; Nix, M. G. D.; Stavros, V. G. *J. Phys. Chem. Lett.* **2010**, *1*, 993-996.
- (10) Kang, H.; Lee, K. T.; Jung, B.; Ko, Y. J.; Kim, S. K. *J. Am. Chem. Soc.* **2002**, *124*, 12958-12959.
- (11) Nix, M. G. D.; Devine, A. L.; Cronin, B.; Ashfold, M. N. R. *J. Chem. Phys.* **2007**, *126*, 124312.
- (12) Kleinerhanns, K.; Nachtigallova, D.; de Vries, M. S. *Int. Rev. Phys. Chem.* **2013**, *32*, 308-342.
- (13) Serrano-Andrés, L.; Merchán, M.; Borin, A. C. *Proc. Natl. Acad. Sci. USA* **2006**, *103*, 8691-8696.

- (14) Barbatti, M.; Aquino, A. J. A.; Szymczak, J. J.; Nachtigallová, D.; Hobza, P.; Lischka, H. *Proc. Natl. Acad. Sci. USA* **2010**, *107*, 21453-21458.
- (15) Barbatti, M.; Lischka, H. *J. Am. Chem. Soc.* **2008**, *130*, 6831-6839.
- (16) Barbatti, M.; Lan, Z.; Crespo-Otero, R.; Szymczak, J. J.; Lischka, H.; Thiel, W. *J. Chem. Phys.* **2012**, *137*, 22A503-514.
- (17) Serrano-Andrés, L.; Merchán, M. *Journal of Photochemistry and Photobiology C: Photochemistry Reviews* **2009**, *10*, 21-32.
- (18) Ludwig, V.; da Costa, Z. M.; do Amaral, M. S.; Borin, A. C.; Canuto, S.; Serrano-Andrés, L. *Chem. Phys. Lett.* **2010**, *492*, 164-169.
- (19) Yamazaki, S.; Kato, S. *J. Am. Chem. Soc.* **2007**, *129*, 2901-2909.
- (20) Conti, I.; Garavelli, M.; Orlandi, G. *J. Am. Chem. Soc.* **2009**, *131*, 16108-16118.
- (21) Chen, J.; Thazhathveetil, A. K.; Lewis, F. D.; Kohler, B. *J. Am. Chem. Soc.* **2013**, *135*, 10290-10293.
- (22) Horke, D. A.; Roberts, G. M.; Lecointre, J.; Verlet, J. R. R. *Rev. Sci. Instrum.* **2012**, *83*, 063101.
- (23) Lecointre, J.; Roberts, G. M.; Horke, D. A.; Verlet, J. R. R. *J. Phys. Chem. A* **2010**, *114*, 11216.
- (24) Horke, D. A.; Verlet, J. R. R. *Phys. Chem. Chem. Phys.* **2011**, *13*, 19546-19552.
- (25) Eppink, A. T. J. B.; Parker, D. H. *Rev. Sci. Instrum.* **1997**, *68*, 3477-3484.
- (26) Roberts, G. M.; Nixon, J. L.; Lecointre, J.; Wrede, E.; Verlet, J. R. R. *Rev. Sci. Instrum.* **2009**, *80*, 053104.
- (27) Adamo, C.; Barone, V. *J. Chem. Phys.* **1999**, *110*, 6158-6170.
- (28) Frisch, M. J.; Trucks, G. W.; Schlegel, H. B.; Scuseria, G. E.; Robb, M. A.; Cheeseman, J. R.; Scalmani, G.; Barone, V.; Mennucci, B.; Petersson, G. A.; Nakatsuji, H.; Caricato, M.; Li, X.; Hratchian, H. P.; Izmaylov, A. F.; Bloino, J.; Zheng, G.; Sonnenberg, J. L.; Hada, M.; Ehara, M.; Toyota, K.; Fukuda, R.; Hasegawa, J.; Ishida, M.; Nakajima, T.; Honda, Y.; Kitao, O.; Nakai, H.;

Vreven, T.; Montgomery, J. A.; Peralta, J. E.; Ogliaro, F.; Bearpark, M.; Heyd, J. J.; Brothers, E.; Kudin, K. N.; Staroverov, V. N.; Kobayashi, R.; Normand, J.; Raghavachari, K.; Rendell, A.; Burant, J. C.; Iyengar, S. S.; Tomasi, J.; Cossi, M.; Rega, N.; Millam, J. M.; Klene, M.; Knox, J. E.; Cross, J. B.; Bakken, V.; Adamo, C.; Jaramillo, J.; Gomperts, R.; Stratmann, R. E.; Yazyev, O.; Austin, A. J.; Cammi, R.; Pomelli, C.; Ochterski, J. W.; Martin, R. L.; Morokuma, K.; Zakrzewski, V. G.; Voth, G. A.; Salvador, P.; Dannenberg, J. J.; Dapprich, S.; Daniels, A. D.; Farkas; Foresman, J. B.; Ortiz, J. V.; Cioslowski, J.; Fox, D. J. Wallingford CT, 2009.

(29) Leang, S. S.; Zahariev, F.; Gordon, M. S. *J. Chem. Phys.* **2012**, *136*, 104101-104112.

(30) Mooney, C. R. S.; Horke, D. A.; Chatterley, A. S.; Simperler, A.; Fielding, H. H.; Verlet, J. R. R. *Chem. Sci.* **2013**, *4*, 921-927.

(31) Gustavsson, T.; Sarkar, N.; Vaya, I.; Jimenez, M. C.; Markovitsi, D.; Improta, R. *Photochemical & Photobiological Sciences* **2013**, *12*, 1375-1386.

(32) Stuhldreier, M. C.; Temps, F. *Faraday Discuss.* **2013**, *163*, 173-188.

(33) Lan, Z.; Lu, Y.; Fabiano, E.; Thiel, W. *ChemPhysChem* **2011**, *12*, 1989-1998.

(34) Mitrić, R.; Werner, U.; Wohlgemuth, M.; Seifert, G.; Bonačić-Koutecký, V. *J. Phys. Chem. A* **2009**, *113*, 12700-12705.

(35) Buchner, F.; Ritze, H.-H.; Lahl, J.; Lubcke, A. *Phys. Chem. Chem. Phys.* **2013**, *15*, 11402-11408.

(36) Chatterley, A. S.; Johns, A. S.; Stavros, V. G.; Verlet, J. R. R. *J. Phys. Chem. A* **2013**, *117*, 5299-5305.

(37) Pluharova, E.; Schroeder, C.; Seidel, R.; Bradforth, S. E.; Winter, B.; Faubel, M.; Slavíček, P.; Jungwirth, P. *J. Phys. Chem. Lett.* **2013**, *4*, 3766-3769.

(38) Su, C.; Middleton, C. T.; Kohler, B. *J. Phys. Chem. B* **2012**, *116*, 10266-10274.

(39) Crespo-Hernandez, C. E.; Cohen, B.; Kohler, B. *Nature* **2005**, *436*, 1141-1144.

(40) Olaso-González, G.; Merchán, M.; Serrano-Andrés, L. *J. Am. Chem. Soc.* **2009**, *131*, 4368-4377.

- (41) Gidden, J.; Bowers, M. T. *Eur. Phys. J. D* **2002**, *20*, 409-419.
- (42) Smith, V. R.; Samoylova, E.; Ritze, H. H.; Radloff, W.; Schultz, T. *Phys. Chem. Chem. Phys.* **2010**, *12*, 9632-9636.
- (43) Doorley, G. W.; Wojdyla, M.; Watson, G. W.; Towrie, M.; Parker, A. W.; Kelly, J. M.; Quinn, S. J. *J. Phys. Chem. Lett.* **2013**, *4*, 2739-2744.

Table of Content (TOC) Graphic

